Fatigue strength improvement of a 4140 steel by gas nitriding: Influence of notch severity

Nathalie Limodin, Yves Verreman

Fatigue strength improvement of a 4140 steel by gas nitriding: influence of notch severity

LIMODIN*, Nathalie and VERREMAN*, Yves

*Department of Mechanical Engineering, Ecole Polytechnique de Montréal, Case Postale 6079, Succursale Centre-ville, Montréal H3C 3A7, Québec, Canada

ABSTRACT

Fatigue failure of a gas-nitrided 4140 steel under axial cyclic loading results from a competition between surface crack initiation in the nitrided case and internal “fish-eye” cracking inside the core material. When nitriding is deep enough, the internal mechanism prevails in smooth specimens and fatigue strength improvement as compared to base metal is about 20%. In the present study, three V-notched specimens (blunt - medium - severe) are designed to be representative of the stress gradient (i) in a small rotary bending specimen, (ii) at the root of a gear tooth, and (iii) at the root of a very sharp notch. The cracking mechanism depends on the notch severity. The nitrided blunt notch fails from a fish-eye nucleated at the case/core boundary whereas the medium and sharp notches fail from surface cracks. The high-cycle fatigue strength improvement varies from 80% for the blunt notch and to more than 100% for the sharp notch. The notch fatigue behaviour of nitrided steel is discussed by comparing the evolutions of internal and surface fatigue strengths with relative stress gradient.

KEYWORDS: Fatigue, AISI 4140 steel, Gas nitriding, notch, stress gradient

INTRODUCTION

Gas nitriding is a thermochemical surface treatment that is used to impart wear, corrosion, and fatigue resistance to service parts. During the gas nitriding treatment, nitrogen, which is provided by the catalytic dissociation of ammonia, diffuses through the part surface to form a concentration gradient as well as nitride precipitates with alloy elements. The saturation of the metal substrate with nitrogen and the nitride precipitates are responsible for hardness increase and for compressive residual stresses in the diffusion layer.

Fatigue tests on nitrided steels are usually performed using smooth specimens under rotary bending. Specimen failure usually occurs from initiation and propagation of an internal “fish-eye” crack. Fatigue strength improvement brought by nitriding can be 50% or more [1,2] which is higher than that measured under uniform axial loading [3]. The stress gradient and the confinement of possible crack initiation sites just below the nitrided layer are the two causes of this overestimation. Rotary bending has several drawbacks including size effect, unconservative strength/life predictions, and impossibility of evaluating mean stress effect.

In a previous study [4,5], the authors performed axial high-cycle fatigue testing of smooth specimens made of gas-nitrided quenched and tempered 4140 steel. The influences of case depth and mean stress were investigated. Fatigue of the nitrided steel is a competition between a surface crack growing in a compressive residual stress field and an internal crack growing in vacuum. A 400µm nitrided case delays crack initiation and growth at the surface, but the improvement of surface fatigue life is small. Shallow case specimens failed from the surface. For nitriding depths of 700µm and more, the improvement of surface fatigue life is large enough for failure to occur always from an internal crack. Unlike bending, there was no evidence that internal fatigue life depends on nitriding depth. “Fish-eye” cracks can initiate and grow anywhere in the core volume and the fatigue strength improvement varies between 15 and 20% depending on the size of the initial defect and the stress level applied.

An interpretation of the minimum nitriding depth necessary to reach the internal fatigue strength level can be made using an elasto-plastic composite model [5]. When the core yields, there is a stress concentration in the elastic case; the thinner the case, the higher this local stress.

The present paper reports a further study from the authors on the notch fatigue behaviour of gas-nitrided 4140 steel. Three notch specimens (blunt, medium and severe notches) were designed to be representative of the stress gradient (i) in a small rotary bending specimen, (ii) at the root of a gear tooth and (iii) at the root of a very sharp notch. Notch effect has been studied using nitrided as well as base metal specimens.

SPECIMENS DESIGN AND STRESS DISTRIBUTIONS

The V-notched specimens (Fig. 1.b to d) were designed with a 90° opening angle and a diameter identical to that of the smooth specimens (Fig. 1.a) to have the same ratio of nitriding depth to diameter. The stress distribution at the notch was computed from finite element analysis for various notch radii [5]. Meshes with six-noded triangular elements were used. They were refined at the notch root to make an accurate computation of the peak stress and of the resultant stress concentration factor K_t; the mesh element size being as small as 10µm at the tip of the sharp notch.

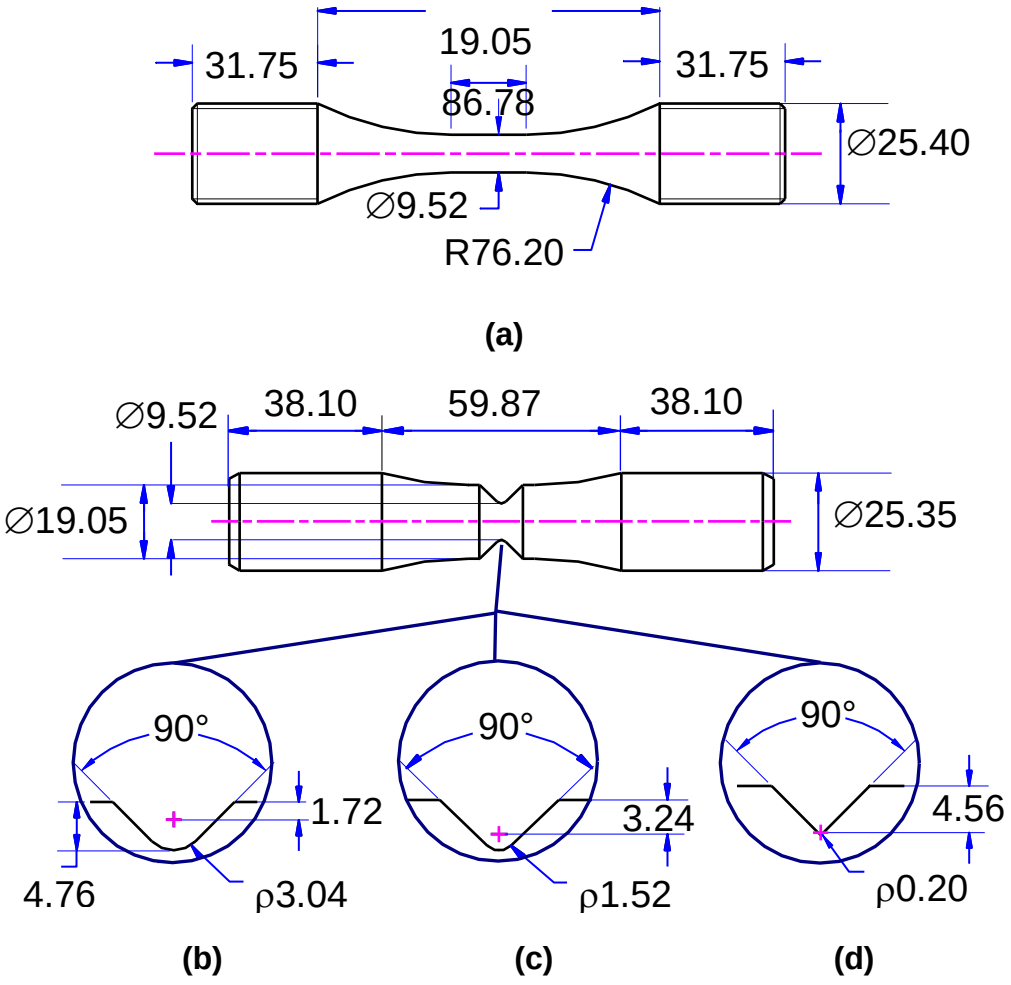

Figure 1: Dimensions in mm of smooth and notched cylindrical specimens used for fatigue testing

The computed axial stress distributions σ_{zz} were normalized by the maximum stress at the notch root, $\sigma_{max} = K_t S$ (Fig. 2). The blunt notch (Fig. 1.b, ρ = 3.04mm) is representative of a rotary bending smooth specimen (Fig. 2). Through the 700µm deep diffusion layer, the normalized

elastic stress distribution is close to the bending applied stress in a 4mm diameter specimen [2,6]. The medium notch (Fig. 1.c) is representative of the root region of a transmission spur gear with 35 teeth and a 140mm pitch diameter; the fillet root radius being equal to 1.52mm if the gear obeys to standard proportions [7]. In literature, the relative stress gradient at a notch root is shown to depend essentially on the notch radius [8,9]. Indeed, the medium notch (ρ = 1.52mm) has a stress distribution that is close to the gear stress distribution computed by Nicoletto [10]. Finally, the sharp notch (Fig. 1.d) represents a poor fatigue design. Its 0.20mm radius is that of the sharpest tool available to machine the notch root.

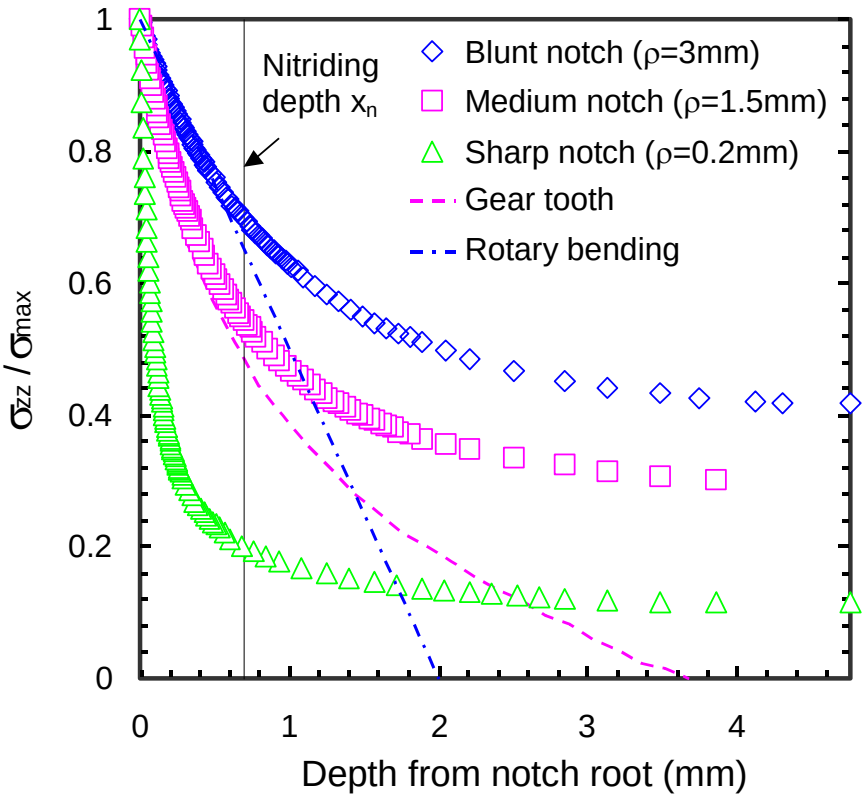

Figure 2: Axial stress distribution at the notch root (stress normalized by the maximum stress)

The stress concentration factor K_t was computed by dividing the maximum axial stress at the notch tip by the nominal stress S computed over the reduced section (Fig. 3). Its value is 1.65 for the blunt notch, 2.11 for the medium notch, and 5.03 for the sharp notch. The corresponding relative stress gradients (Fig. 2)

$$\chi = -\frac{1}{\sigma_{max}} \frac{d\sigma_{zz}}{dx} \qquad \textbf{Eq. 1}$$

are 0.66mm^{-1}, 1.31mm^{-1}, and 9.84mm^{-1}. Because the stress state at the notch root is triaxial, the equivalent stress concentration factor, calculated from Von Mises equivalent stress, is smaller than the uniaxial stress concentration factor K_t, especially when the notch radius is small. The values are 1.5 for the blunt notch, 1.9 for the medium notch, and 4.4 for the sharp notch.

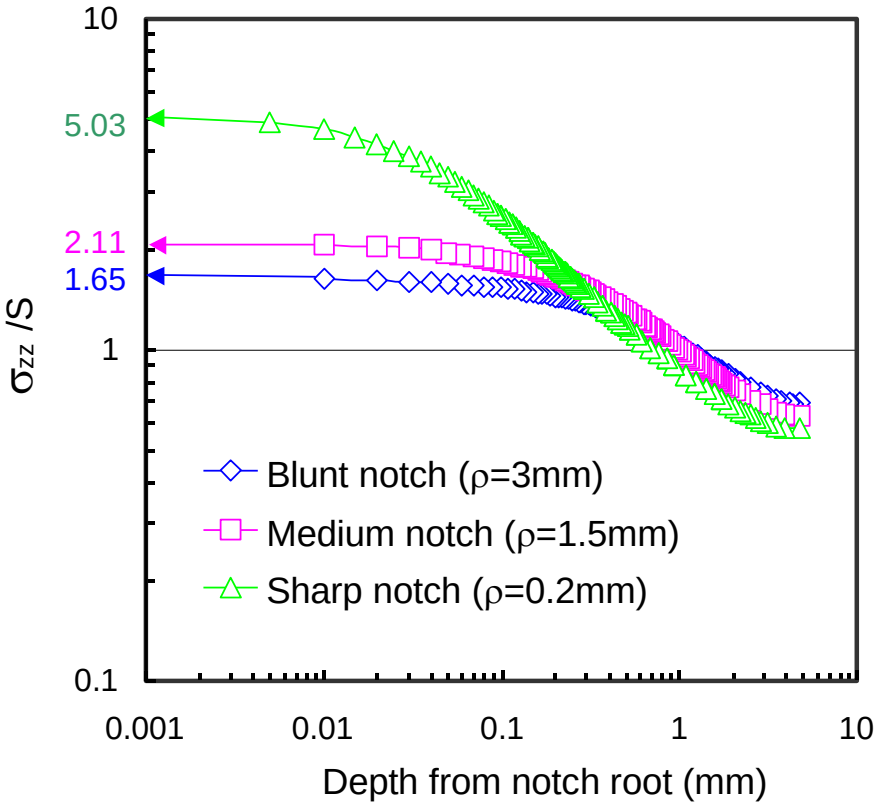

Figure 3: Axial stress distribution at the notch root in log-log coordinates (stress normalized with respect to the nominal stress over minimum section)

EXPERIMENTS

Specimens machining and nitriding

Hot-rolled bars of 4140 steel were quenched and tempered to a hardness of 36HRC. The fatigue specimens were machined and polished according to standard ASTM E466 except for the surface at the notch roots that was left gross of machining. Nitriding was performed in two steps (Table 1). First, the nitriding potential K_N of the atmosphere is high to promote formation of a compound layer at the surface, then, it is strongly decreased while temperature is increased to promote nitrogen diffusion and formation of a diffusion layer. For smooth specimens, the duration of this second step was variable to obtain three nitriding depths, x_n = 400µm, 700µm

and 1000µm (Fig. 4). Some specimens were tested in the as-tempered condition to evaluate the base metal fatigue strength.

Table 1: Details of nitriding treatments

Case depth (µm)	First step	Second step
400	2 h at 500°C $K_N \approx 13$ atm$^{-½}$	2,5 h at 550°C $K_N \approx 0{,}33$ atm$^{-½}$
700		14 h at 550°C $K_N \approx 0{,}33$ atm$^{-½}$
1000		58 h at 550°C $K_N \approx 0{,}33$ atm$^{-½}$

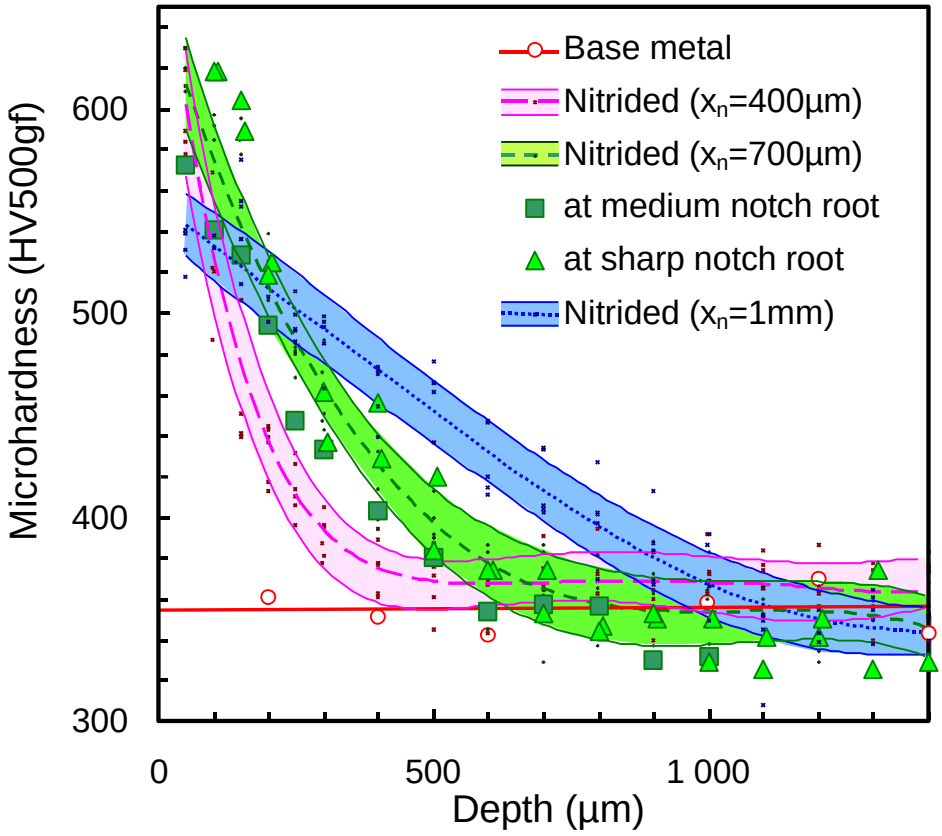

Figure 4: Microhardness profiles with scatter-bands for the three nitriding depths in smooth specimens and microhardness data at medium and sharp notch roots for x_n = 700µm

Nitrided specimens are characterized by a high surface hardness as well as by compressive residual stresses that can reach more than 300MPa at external surface and extend to a depth comparable to the hardening depth [4]. Axial fatigue of nitrided smooth specimens (Fig. 5.a) does not depend on the nitrided case depth when failure occurs by internal “fish-eye” cracking [4]. As shown in Figure 5.a, the 700µm medium case is deep enough to increase the fatigue strength at external surface so that internal cracking in the base metal occurs first.

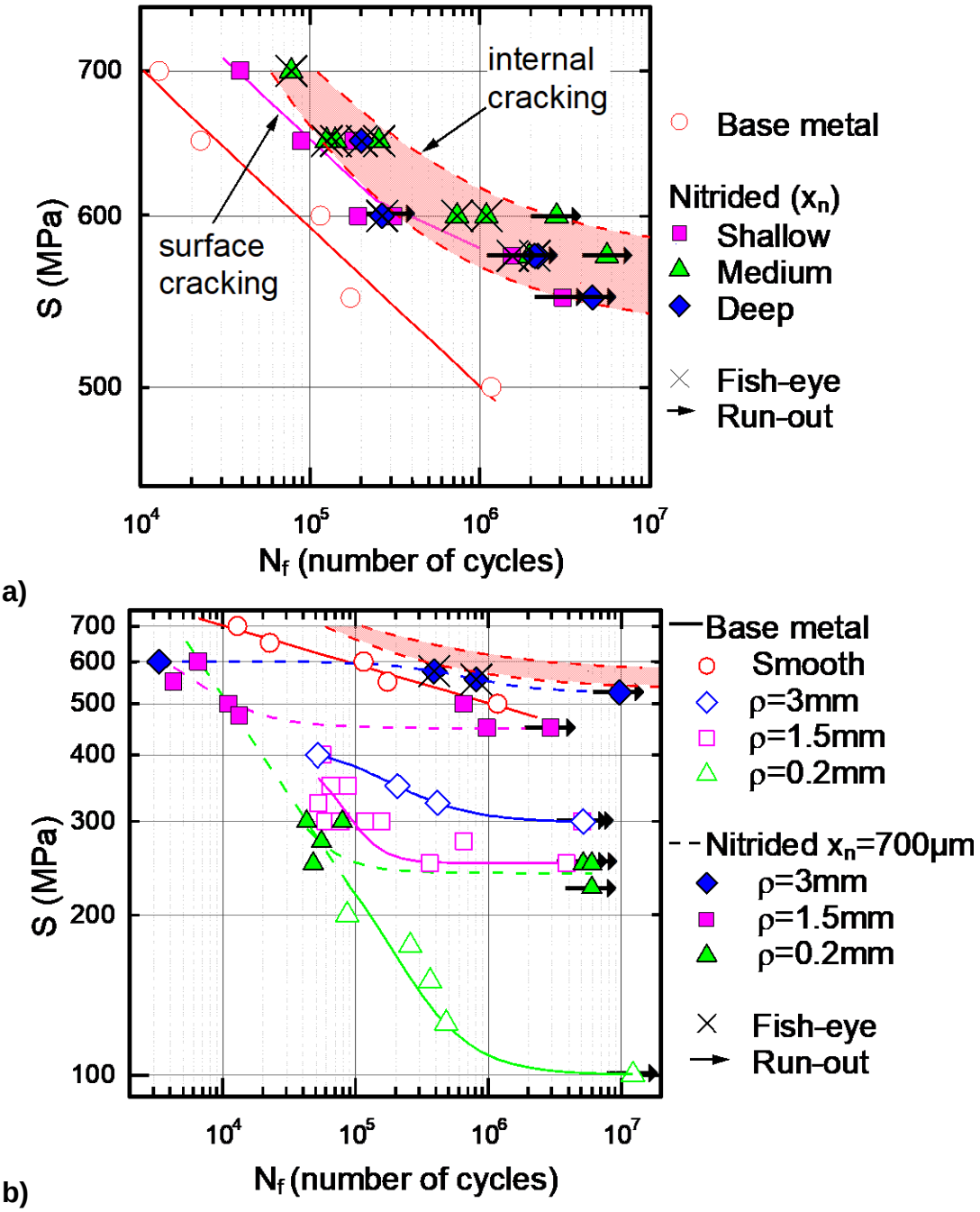

Figure 5: **S-N data obtained from (a) smooth specimens with three nitriding depths and (b) notched specimens with three notch radii**

All notched specimens were tested either in the as-tempered condition or after nitriding to 700µm in depth. Nitriding of a V-notch gave almost the same microhardness profile at the notch tip as that measured in a smooth specimen (Fig. 4). This was verified because the V-notch could disturb the circulation of gases and the nitrogen diffusion inside the material.

Fatigue tests and results

Base metal and nitrided notched specimens were tested under push-pull loading (R = -1) at ambient temperature in laboratory air. Tests were carried out on servo-hydraulic machines (10Hz), and they were run until the sample failure or until five millions cycles. Fracture surfaces were observed first under optical microscope then under SEM. Figure 5.b shows the S-N data for the three notch geometries.

Both internal and external cracking mechanisms were observed in the nitrided steel depending on the notch severity and on the applied stress. For stress levels lower or equal to 575MPa, the blunt notch failed from a fish-eye crack initiated at an inclusion located just under the diffusion layer; however, at 600MPa, it failed from a crack initiated at the surface. Medium and sharp notches always broke by an external cracking mechanism.

In high-cycle fatigue, the notch fatigue strength of the 4140 steel is significantly improved by nitriding. At one million cycles, the fatigue strength improvement was only 20% for smooth specimens. At the same life, it is about 80% for the blunt notch. As far as the internal cracking mechanism is concerned, the (nominal) notch fatigue strength is higher than that of the smooth base metal; it almost merges with the scatter-band associated to internal cracking in smooth specimens.

For the medium notch, the failure is associated to a surface crack and the fatigue strength improvement ranges between 80% and 100%. When the stress gradient is high enough, the surface fatigue strength is always reached before that of the core, and the full advantage of the hardness and the compressive residual stresses of the nitrided case is obtained; nitriding almost compensates for the medium notch effect at long lives. For the sharp notch, the relative improvement of the fatigue strength can exceed 100% at long lives.

Below 10^5 cycles, the fatigue strength improvement is lower whatever the notch. The S-N data fall on a same line while the gap between the base metal and the nitrided steel decreases. At short lives, if plastic deformation occurs below the diffusion case, the stress in the case could be higher than that in elastic design due to stress redistribution between the case and the core. If the local stress reaches the nitrided case strength, the case could break, maybe in static

tension, and the remaining number of cycles before failure would then correspond to crack propagation in the base metal.

In Figure 6, S-N curves were drawn in terms of elastic maximum stresses at the specimen surface, $\sigma_{max} = K_t S$ at the notch root, to interpret the blunt notch results like rotary bending results. At one million cycles, when the same internal cracking mechanism prevails, the strength improvement brought by nitriding is 80% for a stress gradient representative of rotary bending, as compared to 20% for a uniform stress distribution. Rotary bending of small specimens overestimates the fatigue strength of service parts under zero or low stress gradients. Nitriding performs better with a stress gradient because the fish-eye initiates at the vicinity of the case/core boundary where the stress is lower than at the surface. Moreover, with an increasing stress gradient, the probability of having a large defect to initiate a crack decreases as the volume of highly stressed material becomes smaller. Then, the nucleated crack has to grow through a decreasing stress distribution toward the core.

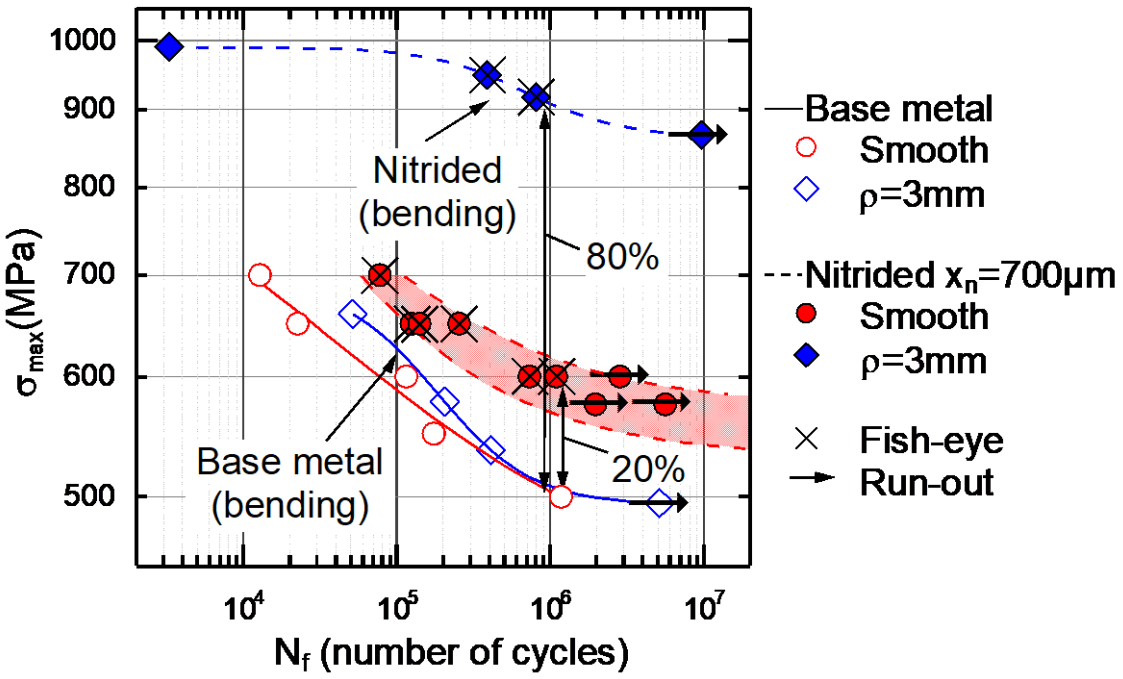

Figure 6: Comparison of fatigue results between tests representative of rotary bending and axial tension-compression tests

Fractographic observations

In the base metal notched specimens, semi-elliptical cracks initiate around the circumference of the notch root where the local stress is the highest. The less severe the notch and, for a given notch, the smaller the applied stress, the fewer are the steps, i.e. the fewer are the nucleated

cracks. At long lives, the fracture surfaces of bluntly notched specimens do not differ much from that of smooth specimens where fracture results from only one initiation site. The scatter in medium notch life at 300MPa (Fig. 5.b) suggests that the fatigue life is still controlled by crack initiation; the more the nucleated cracks, the shorter the fatigue life.

At the sharp notch, tiny steps are spread all around the notch root indicating that many cracks easily nucleated then rapidly formed a circumferential crack. A specimen that did not break after 10^7 cycles at 100MPa was hold at maximum stress and coated with Indian ink to mark a potential crack at the notch root. Then, it was re-tested at 200MPa where it broke after 86,000 cycles. Scanning electron micrographs (Fig. 7) reveal a surface contamination, which extends from 10 to 30µm in depth and covers almost the entire circumference. This could correspond to a non-propagating crack; the 100MPa stress was enough to initiate a crack but not to propagate it farther than 30µm.

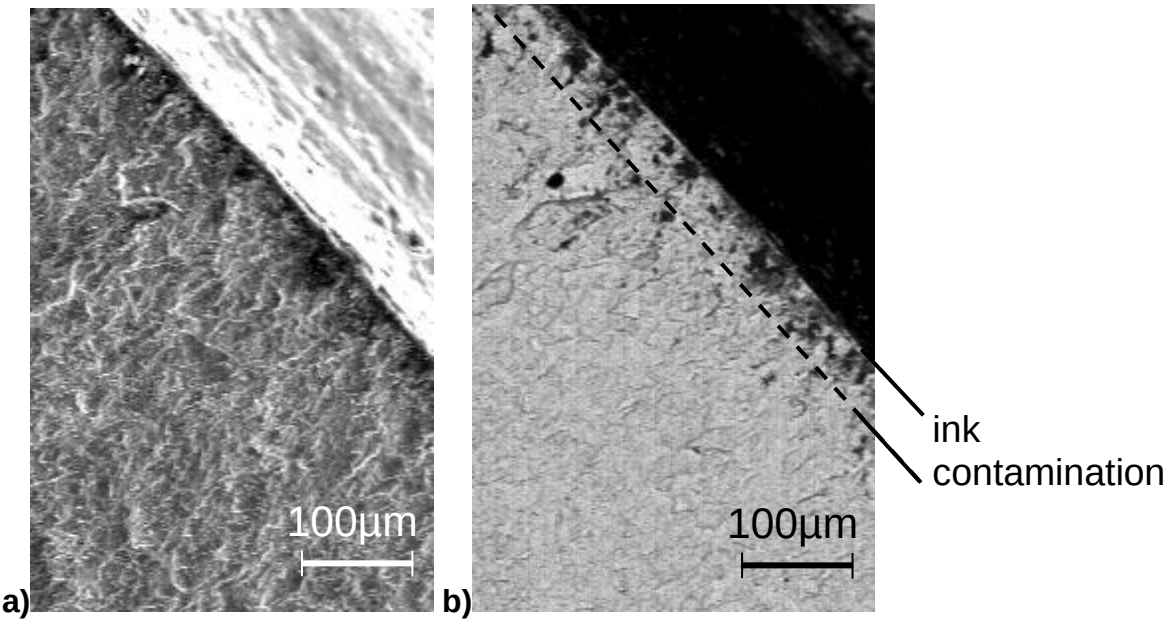

Figure 7: SEM fractographs in (a) topographic and (b) composition modes of a possible non-propagating crack at the sharp notch

Nitrided blunt notches have failed by an internal cracking mechanism at 575MPa and below (Fig. 8). Beneath the blunt notch root, fish-eye cracks initiate at oxide inclusions (Ca, Al, S, O) that are about 20µm in diameter; they could be as deep as 2mm though only those that nucleated close to the case/core boundary grew into a fatal crack. Apart from the initiation site localisation, the internal cracking mechanism resembles that already observed in smooth specimens [4]. A crack initiates at an inclusion and propagates slowly in a vacuum-like environment. When the fish-eye grows deep enough in the nitrided case, a large surface crack

forms and propagates rapidly until final fracture at the opposite side. At 600MPa, the notch root stress is high enough to nucleate and propagate a crack at the nitrided surface before a fish-eye crack nucleated at 970µm in depth has the possibility to grow.

Nitrided medium and sharp notches have always failed from cracks initiated at the external surface whatever the stress level. The final fracture zone was larger in the nitrided steel than in the base metal because a higher stress has to be applied. At the notch root, cracks nucleate at some points before they probably cause a static failure of the nitrided case over a large arc. An annular fatigue crack then grows quickly in the core with deep radial marks showing much more plastic deformation than in the hard case. Whatever the notch severity, the broken nitrided case presents two zones of different topography (Fig. 9.a). Beneath the flat fracture surface of the white layer (about 10µm), the most superficial zone (200-400 µm) of the diffusion case is granular (Fig. 9.b); it is a mixture of intergranular cracking and quasi-cleavage. Then there is a smooth transition zone that extends to the end of the diffusion case before the typical quasi-cleavage topography of base metal is observed.

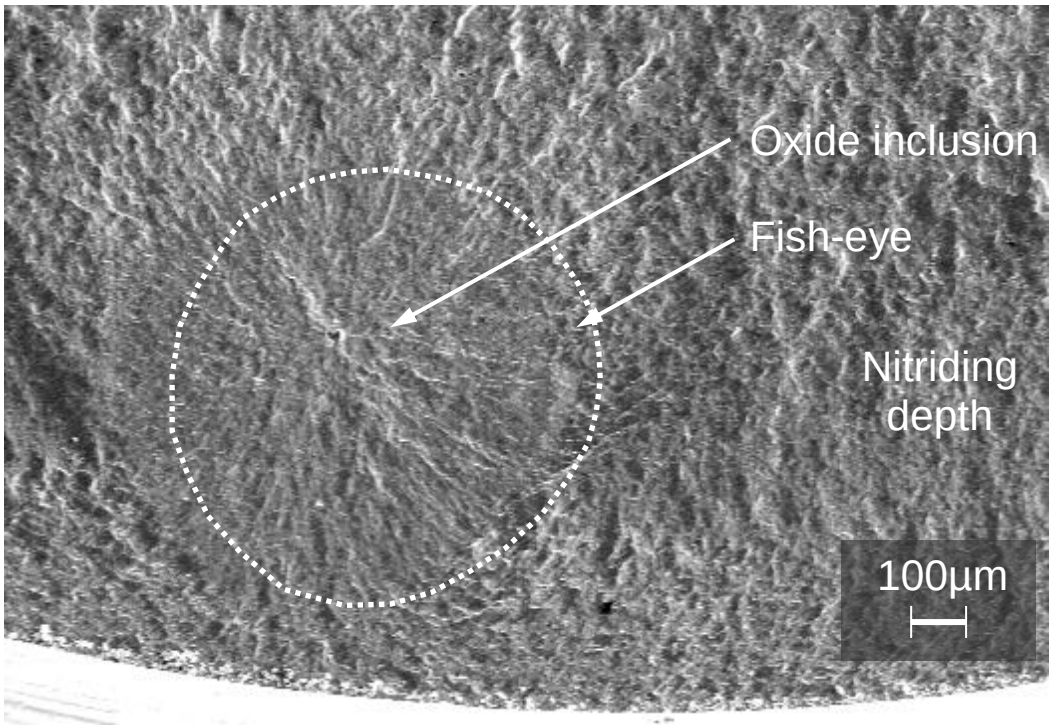

Figure 8: Fish-eye crack nucleated under the diffusion layer at a nitrided blunt notch (575MPa, 389,216 cycles)

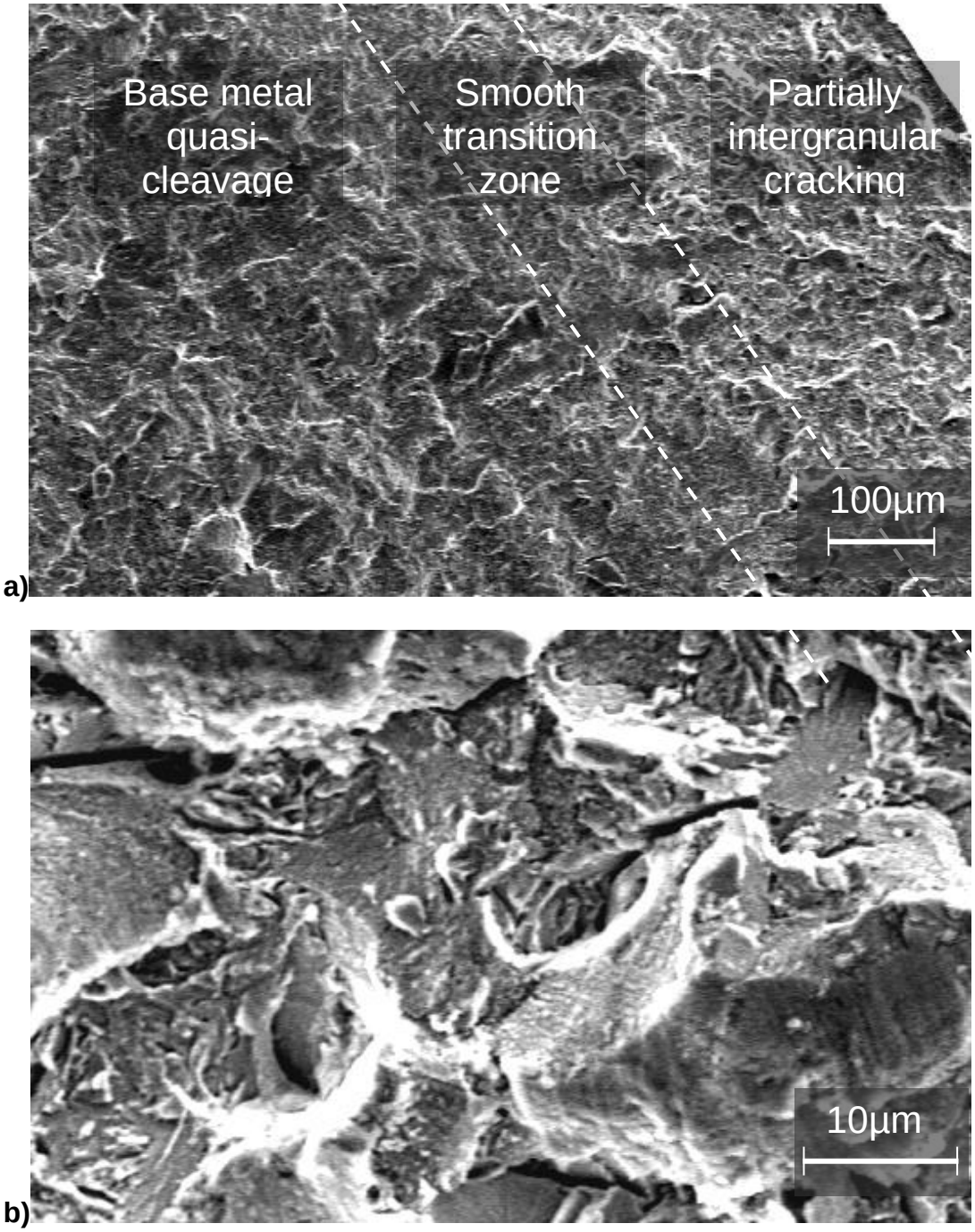

Figure 9: (a) Surface cracking at a nitrided medium notch broken after 971,998 cycles at 450MPa with (b) a magnification of the intergranular cracking zone

The granular aspect of the superficial zone of the broken case could correspond to a quasi-static brittle fracture similar to what was observed in tensile testing [5]; the local stresses at medium and sharp notch roots exceed 1000MPa. The harmful effect of an overload was observed (Fig. 10). A medium notch tested at 450MPa, was overloaded at 2.944 million cycles and broke about 8,000 cycles later. Many steps appear all around the notch circumference and

the final fracture occurs almost at the centre of the specimen. The overload, which is 175% higher than the constant applied stress, obviously damaged the nitrided layer that broke in a brittle manner so that the remaining life corresponds to the propagation life in the base metal.

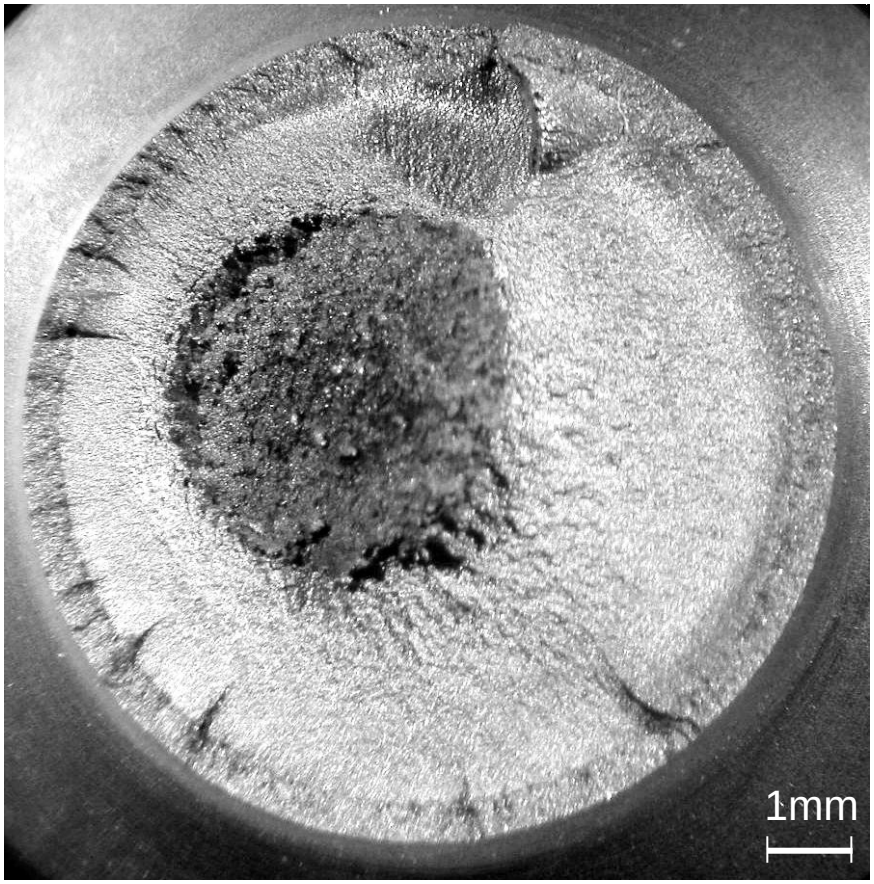

Figure 10: Nitrided medium notch broken after 2.952 millions cycles at 450MPa after an overload at 2.944 millions cycles

DISCUSSION

Notch behaviour of base metal

When the notch radius decreases, the slope of the base metal S-N curve increases (Fig. 4b) suggesting that the sharper the notch, the larger the fraction of fatigue life that is spent in crack propagation. The S-N curve slope of smooth specimens is -0.073 while that of sharp notches is of -0.247. This is close to -1/m = -0.297 where m is the Paris' law coefficient measured for this material [5].

The base metal cyclic yield stress is about 600MPa according to data published for a comparable material [11]. FE calculations of the Von Mises' equivalent stress distribution show that no plastic zone develops at the blunt notch root below 400MPa. However, plastic zones develop at the medium and sharp notches for nominal stresses larger than 316MPa (8.10^4 cycles) and 137MPa (4.10^5 cycles) respectively. In such conditions, crack initiation life can become negligible as compared to propagation life. Note that, for nominal stress higher than 300MPa, the medium notch S-N curve becomes steeper while the life scatter decreases. On the other hand, near the endurance limit, the fatigue life is dominated by crack initiation and it is sensitive to the number and harmfulness of the defects at the notch root.

Various empirical methods are proposed to predict the notch effect. The Juvinall method described in Dowling's book [12] estimates the Wöhler curve of smooth specimens from the material tensile strength, the loading type, the surface finish, and the diameter. Then, to predict the notch fatigue curve (Fig. 11), the fatigue limit and the fatigue strength at 1,000 cycles are divided by a fatigue notch factor K_f computed from the empirical Neuber's formula. Full notch sensitivity corresponds to the case where $K_f = K_t$, i.e. the notch fatigue limit is equal to the smooth surface fatigue limit divided by K_t:

$$S_D^{notch} = \frac{S_D^{smooth}}{K_t} \qquad \textbf{Eq. 2}$$

The quenched and tempered 4140 base metal is more notch sensitive than mild steels. As shown in Figure 11, the long life fatigue strengths of blunt and medium notches are relatively well correlated by equation (2). However, those of sharp notches are underestimated. The Juvinall method gives better estimates but it does not consider crack propagation life.

Notch behaviour of nitrided steel

Figure 12 presents data and predictions of fatigue strengths at 10^6 cycles versus stress concentration factor K_t and relative stress gradient χ. The external fatigue strength of the nitrided notched steel can be estimated by equation (2) as well as that of the base metal. The smooth surface fatigue strength has been computed using the fatigue strength measured for the medium notch multiplied by the stress concentration factor K_t ($S_D^{smooth} \approx$ 1,000MPa instead of 500MPa for the base metal). The fatigue strength at one million cycles of the sharp nitrided notch is between 250 and 275MPa, i.e. it is more than twice that of the base metal. In addition to an improvement of the resistance to crack initiation, the critical stress for crack propagation could also be higher in the nitrided steel because of the influence of compressive residual stresses on crack closure.

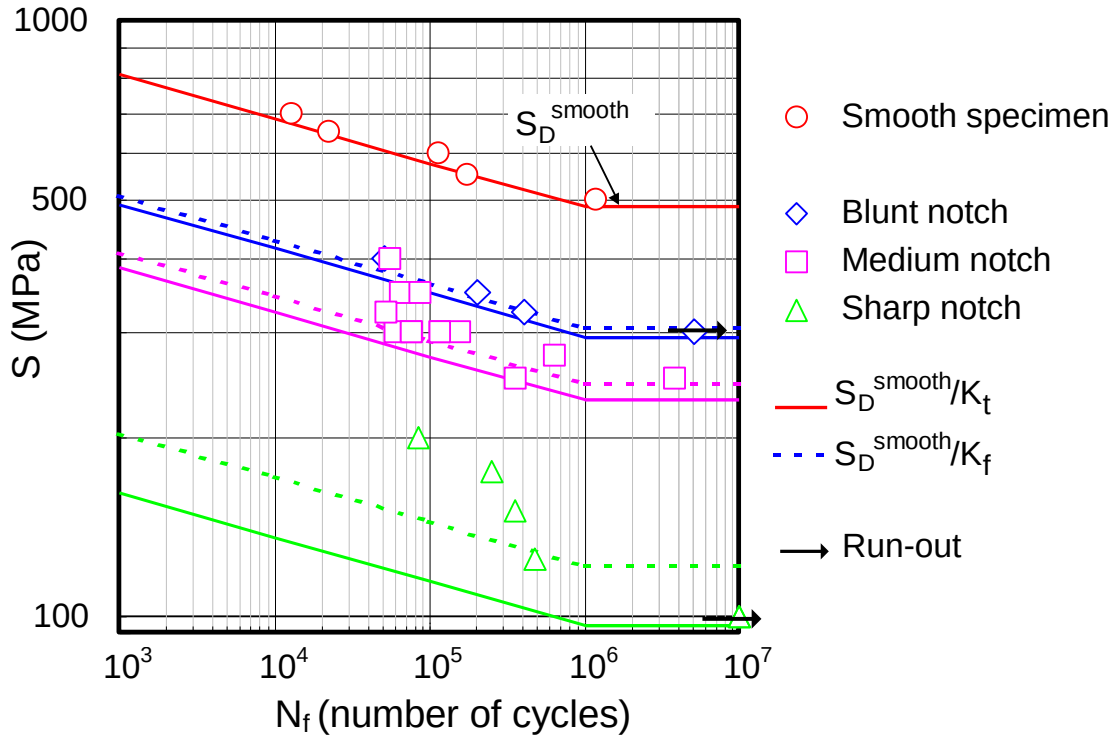

Figure 11: Life predictions versus S-N data for the base metal

The internal fatigue strength $S_{D\_\text{int}}^{notch}$ can be estimated by assuming that the fish-eye crack initiates at the nitriding depth (x = x_n) when the local stress $\sigma_{zz}(x = x_n)$ reaches the internal fatigue strength $S_{D\_\text{int}}^{smooth} = 600\text{MPa}$ as measured on smooth specimen,

$$S_{D\_\text{int}}^{notch} = \frac{S_{D\_\text{int}}^{smooth}}{K_t \times f(x_n)} \qquad \textbf{Eq. 3}$$

where f(x)≤1 is the normalized stress distribution shown in Fig. 2. For a relative depth x/ρ smaller than 0.3, this distribution can be written as a function of x/ρ,

$$f(x) = 1 - 2\frac{x}{\rho} + 2.6\left(\frac{x}{\rho}\right)^2 \qquad \frac{x}{\rho} \le 0.3 \qquad \textbf{Eq. 4}$$

The predicted internal fatigue strength is drawn in Figure 12 for x_n = 0.7mm under the notch root; the shaded zone corresponding to the scatter-band of smooth specimens (Fig. 4a). Initially, the internal fatigue strength slightly decreases when the stress gradient increases. Then, for higher stress gradient, the $K_t \times f$ product tends to unity (the under-layer stress tends to the

nominal stress) and the internal fatigue strength re-increases to the level of smooth specimens. Note that, in bending, the internal fatigue strength would be larger for a notched part than for a smooth part, and that it would increase with stress gradient [13].

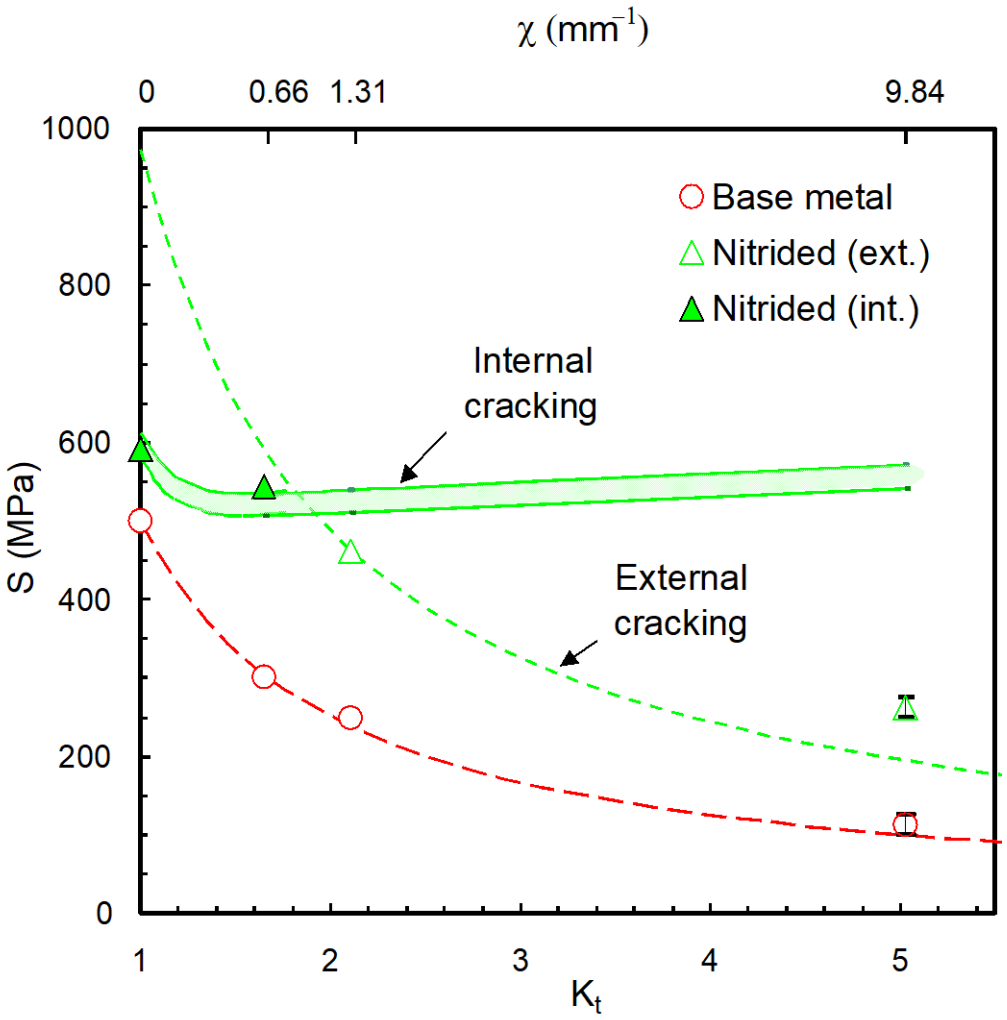

Figure 12: Fatigue strength at 10^6 cycles versus stress concentration factor K_t and relative stress gradient χ

The curves of internal and external fatigue strengths intersect for a notch geometry that is intermediate between the blunt and medium notches. There is a relative stress gradient χ for which internal and external cracking are equi-probable. At one million cycles, the ratio of external to internal fatigue strengths is:

$$\frac{S_{D-ext}^{notch}}{S_{D-\text{int}}^{notch}} = \frac{1000}{600} f(x_n) \qquad \textbf{Eq. 5}$$

Using equation (4) and replacing the notch radius ρ by the relative stress gradient at $x = 0^+$,

$$\chi = -f'(x) = \frac{2}{\rho} \qquad \textbf{Eq. 6}$$

equation (5) becomes

$$\frac{S_{D-ext}^{notch}}{S_{D-\mathrm{int}}^{notch}} = 1.66 - 1.66(x_n\chi) + 1.079(x_n\chi)^2 \qquad x_n\chi \le 0.6 \qquad \textbf{Eq. 7}$$

For a given nitriding depth (x_n = 0.7mm in this study), the strength ratio continuously decreases with increasing stress gradient χ even beyond the validity limit of equation (7). The transition from internal to external cracking occurs when the strength ratio becomes smaller than unity. The critical stress gradient is about 0.86mm^{-1}. At the blunt notch (χ = 0.66mm^{-1}), the internal cracking mechanism still prevails. At the medium notch (χ = 1.31mm^{-1}), the internal cracking mechanism requires a higher stress than the external mechanism so that the latter now prevails. The fatigue strength improvement brought by nitriding is maximized when the internal fatigue strength becomes larger than the external one.

The model developed here is purely elastic and it neglects the stress redistribution between the case and the core when the core deforms plastically. The cyclic yield stress of the core (600MPa) is not reached at sharp and medium notches when the stress at surface reaches 1,000MPa (Fig. 2). On the other hand, at the blunt notch, there can be a macroscopic plastic deformation under the nitrided layer. A better description of the fatigue behaviour of blunt notches would be obtained with an elasto-plastic model, which considers the composite nature of the nitrided steel.

CONCLUSIONS

The notch fatigue behaviour of a nitrided 4140 steel was explored using cylindrical V-notched specimens under fully reversed axial loading (R = -1). The nitriding depth (700µm) was large enough for failure of smooth specimens to occur from an internal (fish-eye) crack in the base metal. Three notch geometries (blunt - medium - severe) were designed to be representative of the stress gradient (i) in a small rotary bending specimen, (ii) at the root of a gear tooth, and (iii) at the root of a very sharp notch. The stress concentration factors K_t are 1.65, 2.11, and 5.03 respectively and the relative stress gradients are 0.66mm^{-1}, 1.31mm$^{-1,}$ and 9.84mm^{-1}. The main conclusions are the following.

1. The quenched and tempered base metal is notch sensitive. In high cycle fatigue, blunt and medium notch fatigue strengths are well correlated by the stress concentration factor K_t. However, the behaviour of severe notch is controlled by crack propagation. Non-propagating cracks were highlighted on a fracture surface.

2. The fatigue strength improvement brought by nitriding increases rapidly from 20% to 80% when the stress gradient varies from zero (smooth axially-loaded specimen) to 0.66mm^{-1} (blunt notch equivalent to rotary bending specimen). The S-N curve of the nitrided blunt notch lies above that of base metal smooth specimen. Fish-eye crack initiation under the nitrided layer requires high nominal stress.

3. Beyond a critical stress gradient (evaluated to 0.86mm^{-1} in the present study), fatigue failure occurs from external cracking before the internal fatigue strength is reached. The relative fatigue strength improvement with respect to base metal is maximum (= 100% or more). Nitriding almost compensates for the notch effect in the specimen representative of the root of a gear tooth (radius = 1.52mm).

4. Quasi-static brittle fracture of the nitrided layer is observed above the fatigue limit, so that the fatigue life reduces to the crack propagation life at a high stress level in the base metal. Further investigation should be made on the sensitivity to static overloads.

ACKNOWLEDGEMENTS

We acknowledge Nitrex Metal Inc. and National Research Council of Canada for their support.

REFERENCES

1 Y. Sun, T. Bell, Materials Science and Engineering A 140 (1991) 419-434.

2 K. Genel, M. Demirkol, M. Capa, Materials Science and Engineering A 279 (2000) 207-216.

3 J.M. Cowling, Fatigue Behaviour of Nitrided Steel. Strength of Metals and Alloys. Pergamon Press, Oxford, 1983.

4 N. Limodin, Y. Verreman, T.N. Tarfa, Fatigue and Fracture of Engineering Materials and Structures 26 (2003) 811-820.

5 N.Limodin, Amélioration de la résistance en fatigue d'un acier 4140 par nitruration gazeuse. Ph.D. Dissertation, Ecole Polytechnique de Montreal (2005).

6 T. Bell, N.L. Loh, Journal of Heat Treating 2 (1982) 232-237.

7 D.W. Dudley, Handbook of Practical Gear Design, Mc Graw-Hill Book Company, New York, 1984.

8 J. Schijve, Fatigue of Engineering Materials and Structures 3 (1980) 325-338.

9 B. Atzori, P. Lazzarin, S. Filippi, International Journal of Fatigue 23 (2001) 355-362.

10 G. Nicoletto, Engineering Fracture Mechanics 44 (1993) 231-242.

11 T. Bruder and T. Seeger, Materialwissenschaft und Werkstofftechnik 26 (1995) 89-100.

12 N.E. Dowling, Mechanical Behavior of Materials - Engineering Methods for Deformation, Fracture, and Fatigue, Prentice Hall, Englewood Cliffs, 1993.

13 H.J. Spies, T.U. Kern, and N.D. Tan, Materialwissenschaft und Werkstofftechnik (Germany) 25 (1994) 191-198.